The University of San Francisco

USF Scholarship: a digital repository @ Gleeson Library | Geschke Center

Mathematics   College of Arts and Sciences

Stability and Clustering of Self-Similar Solutions of Aggregation Equations

Hui Sun

David Uminsky
University of San Francisco, duminsky@usfca.edu

Andrea L. Bertozzi

Follow this and additional works at: http://repository.usfca.edu/math

Part of the Mathematics Commons, and the Physics Commons

Stability and clustering of self-similar solutions of aggregation equations

Hui Sun,[1,a)] David Uminsky,[2,b)] and Andrea L. Bertozzi[1,c)]

[1]*Department of Mathematics, UCLA, Box 951555, Los Angeles, California 90095-1555, USA*
[2]*Department of Mathematics, University of San Francisco, 2130 Fulton Street, San Francisco, California 94117-1080, USA*

In this paper we consider the linear stability of a family of exact collapsing similarity solutions to the aggregation equation $\rho_t = \nabla \cdot (\rho \nabla K * \rho)$ in $\mathbb{R}^d$, $d \geq 2$, where $K(r) = r^\gamma/\gamma$ with $\gamma > 2$. It was previously observed [Y. Huang and A. L. Bertozzi, "Self-similar blowup solutions to an aggregation equation in Rn," J. SIAM Appl. Math. **70**, 2582–2603 (2010)] that radially symmetric solutions are attracted to a self-similar collapsing shell profile in infinite time for $\gamma > 2$. In this paper we compute the stability of the similarity solution and show that the collapsing shell solution is stable for $2 < \gamma < 4$. For $\gamma > 4$, we show that the shell solution is always unstable and destabilizes into clusters that form a simplex which we observe to be the long time attractor. We then classify the stability of these simplex solutions and prove that two-dimensional (in-)stability implies n-dimensional (in-)stability. © *2012 American Institute of Physics.* [http://dx.doi.org/10.1063/1.4745180]

Dedicated to Peter Constantin of the occasion of his 60th birthday.

I. INTRODUCTION

In this paper, we consider the active scalar equation:

$$\rho_t = \nabla \cdot (\rho \nabla (K * \rho)) \qquad \text{in } \mathbb{R}^d, \tag{1}$$

where ρ is the active scalar, $*$ denotes convolution, and K is a potential function. This equation arises in many applications such as swarming of animal flocks,[2–9] chemotaxis,[10–12] self-assembly of nanoparticles,[13,14] and granular flow,[15–19] to name just a few. Recently, the finite time blow up problem of (1) has drawn much attention. The existence and uniqueness of solutions for rough initial data and singular potential K has been proven for both one dimension[2,4] and n space dimensions.[20] Finite-time blow-up of solutions under rotationally symmetric kernels with a Lipschitz point at the origin is also known.[21,22] For weak measure solutions the well-posedness theory, uniqueness, and global existence has been recently been explored.[23,24] An Osgood condition on the kernel which is a necessary and sufficient condition for finite time blow up has also been derived.[25,26] For power law kernels

$$K(r) = \frac{r^\gamma}{\gamma}, \tag{2}$$

the critical power is $\gamma = 2$ for finite vs. infinite time blow up.[25] Blow up of solutions exhibit self similarity which has been demonstrated numerically[1,27] by Huang and Bertozzi for radially symmetric solutions. In particular they show that symmetric initial conditions blow up at the origin in a self-similar way in finite time for $\gamma < 2$; while it collapses to a delta shell in a self-similar way in infinite time for $\gamma > 2$.

a)E-mail: huiprobable@math.ucla.edu.
b)E-mail: duminsky@usfca.edu.
c)E-mail: bertozzi@math.ucla.edu.

We consider the case $\gamma > 2$ in $\mathbb{R}^d$, where the delta shell solution has been shown to be an attractor under the self-similar collapse in the space of radially symmetric solutions.[1,27] Stability of self-similar solutions has been investigated for gravitational collapse and star formation,[28–30] pinchoff in surface diffusion,[31] as well as chemotactic collapse,[11,32,33] and is a problem of general interest. After rewriting Eq. (1) in self-similar variables, the aggregation kernel (2) has a local repulsion and global attraction structure. Numerical simulations[24,34–36] of (1) with this repulsion-attraction structure yield uniformly distributed shell solutions as well as a rich diversity of both radially and non-radially symmetric ground states. In previous work,[34,35] stability analysis has been used to accurately predict which patterns will arise from the gradient flow dynamics.

Using the stability analysis of shell solutions we find that there is a regime of stability in which the collapsing shell solution is still an attractor and a regime where the shell solution becomes unstable. In the unstable case, solutions aggregate not on a shell profile but cluster to the more singular simplex solution, for example the vertices of an equilateral triangle (in $\mathbb{R}^2$) or a regular tetrahedron (in $\mathbb{R}^3$). The clustering problem for general space dimensions is related to the question of sphere packing. Many researchers have discovered various configurations on a sphere that minimize specific energies. In particular, Cohn and Kumar derive the universal optimality of sharp configurations,[37] stating that sharp configurations minimize the energy defined by $\sum_{x,y \in \mathcal{C}} \phi(|x - y|^2)$, with $\phi : (0, 4] \to \mathbb{R}$ s.t. $\phi \in C^\infty$ and $(-1)^k \phi^{(k)} \geq 0$ for all k, where $\mathcal{C}$ is a finite collection of points on the unit sphere. However, their work is done for purely repulsive potentials ϕ while restricting the domain of the particles to a sphere, whereas we consider the free space problem where our potential has both repulsion and attraction.

To perform this analysis we begin in Sec. II by deriving a weak formulation of Eq. (1) where the solutions are supported on a $d - 1$ dimensional manifold which follows the derivations found here.[35] In Sec. III, we analytically derive simple conditions for the stability of shell solutions for general, *non-radially* symmetric perturbations. We also investigate the form of the long time solutions in $\mathbb{R}^2$ and observe that, in the regime of instability, the ring breaks up into a finite number of clusters distributed around the center of mass. Under general perturbations, the distribution is generically an equilateral triangle and a simplex in higher dimensions. In Sec. IV we first derive stability conditions for cluster solutions in $\mathbb{R}^2$ and then derive simple conditions for when $\mathbb{R}^2$ simplex (in-)stability implies $\mathbb{R}^d$ simplex (in-)stability. We provide concluding remarks and future work in Sec. V.

II. WEAK FORMULATION OF THE PROBLEM

In this section, we apply the similarity transformation as discussed in Refs. 1 and 27, and then derive the evolution equations for the solution to (1) and (2) concentrating on a co-dimension one manifold. We remark here that this weak formulation generalizes the classical Birkhoff-Rott equation in two dimensions,[38] and has been extended to general dimensions[24,35] to study the stability of ground states which aggregate on co-dimension one manifolds.

To begin, we rewrite the system (1) and (2) as:

$$\mathbf{x}_t = \mathbf{u} = -\int_{\mathbb{R}^d} K'(|\mathbf{x} - \mathbf{x}'|)\frac{\mathbf{x} - \mathbf{x}'}{|\mathbf{x} - \mathbf{x}'|}\rho(\mathbf{x}')\mathrm{d}\mathbf{x}' \tag{3}$$

$$\rho_t = -\nabla \cdot (\rho\mathbf{u}), \tag{4}$$

where $\mathbf{x} \in \mathbb{R}^d$, $\mathbf{u}$ is the velocity at any point $\mathbf{x} \in \mathbb{R}^d$, and $K'(r) = r^{\gamma - 1}$. We define the similar variables

$$\mathbf{y} = \mathbf{x}t^\beta, \quad \tau = \ln t, \quad p = t^\alpha \rho,$$

$$\text{with } \alpha = \frac{n}{\gamma - 2} \text{ and } \beta = \frac{1}{\gamma - 2} \tag{5}$$

which leads to the following set of equations:

$$\mathbf{y}_\tau = \mathbf{v}$$

$$= \int_{\mathbb{R}^d} (\beta |\mathbf{y} - \mathbf{y}'| - K'(|\mathbf{y} - \mathbf{y}'|)) \frac{\mathbf{y} - \mathbf{y}'}{|\mathbf{y} - \mathbf{y}'|} p(\mathbf{y}') \mathrm{d}\mathbf{y}', \tag{6}$$

$$p_\tau = -\nabla \cdot (p\mathbf{v}). \tag{7}$$

Remark: We note here that the similarity transformation has resulted in our new evolution equations (6) and (7) to have a repulsion-attraction interaction kernel, $\beta |\mathbf{y} - \mathbf{y}'| - K'(|\mathbf{y} - \mathbf{y}'|)$. This has the effect of fixing the collapsing $\mathcal{S}^{d-1}$ solutions to be frozen and we can then study the stability of these constant states.

The solutions we consider are co-dimension one and thus the density concentrates on a surface. We parameterize the surface with Lagrangian parameter $\boldsymbol{\xi} \in D \subset \mathbb{R}^{d-1}$, and denote the material point position on the surface as $\mathbf{Y}(\boldsymbol{\xi})$; Eqs. (6) and (7) reduce to:

$$\mathbf{Y}_\tau = \mathbf{v}$$

$$= \int_D (\beta |\mathbf{Y} - \mathbf{Y}'| - K'(|\mathbf{Y} - \mathbf{Y}'|)) \frac{\mathbf{Y} - \mathbf{Y}'}{|\mathbf{Y} - \mathbf{Y}'|} P(\boldsymbol{\xi}', \tau) \mathrm{d}\mathcal{S}_{\boldsymbol{\xi}'} \tag{8}$$

$$P_\tau(\boldsymbol{\xi}, \tau) = 0, \tag{9}$$

where the density $P(\boldsymbol{\xi}, \tau)$ has the weak formulation:

$$p(\mathbf{y}, \tau) = \int_D \delta(\mathbf{y} - \mathbf{Y}(\boldsymbol{\xi}', \tau)) P(\boldsymbol{\xi}', \tau) \mathrm{d}\boldsymbol{\xi}'. \tag{10}$$

Equation (9) implies $P(\boldsymbol{\xi}, \tau) = P(\boldsymbol{\xi}, 0)$. Hence Eq. (8) can be written as

$$\mathbf{Y}_\tau = \mathbf{v}$$

$$= \int_D (\beta |\mathbf{Y} - \mathbf{Y}'| - K'(|\mathbf{Y} - \mathbf{Y}'|)) \frac{\mathbf{Y} - \mathbf{Y}'}{|\mathbf{Y} - \mathbf{Y}'|} P_0(\boldsymbol{\xi}') \mathrm{d}\mathcal{S}_{\boldsymbol{\xi}'}, \tag{11}$$

where $P_0(\boldsymbol{\xi})$ is the initial density. Note that one can approximate Eq. (11) by replacing the continuous density function as a discrete set of particles $\{\mathbf{Y}(\boldsymbol{\xi}_i) : i = 1, 2, \ldots, N\}$ scattering on the surface $\{\mathbf{Y}(\boldsymbol{\xi}) : \boldsymbol{\xi} \in D\}$ with mass $\{m_i = p_0(\boldsymbol{\xi}_i)\Delta\boldsymbol{\xi}_i : i = 1, 2, \ldots, N\}$, where $\{\boldsymbol{\xi}_i, \Delta\boldsymbol{\xi}_i\}$ defines the partition of D. With the notation $\mathbf{Y}_i = \mathbf{Y}(\boldsymbol{\xi}_i)$, we arrive at the following discretized particle interaction equation:

$$\dot{\mathbf{Y}}_j = \mathbf{v} = \frac{1}{N} \sum_{k \neq j} f(|\mathbf{Y}_j - \mathbf{Y}_k|) \frac{\mathbf{Y}_j - \mathbf{Y}_k}{|\mathbf{Y}_j - \mathbf{Y}_k|} m_k \tag{12}$$

with the same interacting kernel

$$f(|\mathbf{Y}_j - \mathbf{Y}_k|) = \beta |\mathbf{Y}_j - \mathbf{Y}_k| - K'(|\mathbf{Y}_j - \mathbf{Y}_k|). \tag{13}$$

The continuous equation (11) allows for linear stability analysis, while the discrete equation (12) provides a straightforward method for simulating the fully nonlinear problem. For simplicity of analysis, we assume the particles are equally weighted, i.e, $m_k = 1 \; \forall \; k$.

III. LINEAR STABILITY OF SHELL SOLUTIONS

A. Linear stability of shell solution in $\mathbb{R}^d$

In this section, we analyze the stability of shell solutions, hereby denoted as $\mathcal{S}^{d-1}$, with constant initial density, i.e, $P_0(\boldsymbol{\xi}) = 1$. Recall that in $\mathbb{R}^d$, the distance between two vectors on a sphere $|\mathbf{Y} - \mathbf{Y}'|$ can be related to their inner product through the following formula:

$$|\mathbf{Y} - \mathbf{Y}'|^2/2 = R^2 - \mathbf{Y} \cdot \mathbf{Y}',$$

$$\text{given } |\mathbf{Y}| = |\mathbf{Y}'| = R. \tag{14}$$

For convenience, we rewrite (11) as:

$$\mathbf{Y}_\tau = \mathbf{v} = \int_D g\left(\frac{|\mathbf{Y}-\mathbf{Y}'|^2}{2}\right)(\mathbf{Y}-\mathbf{Y}')\mathrm{d}\mathcal{S}_{\xi'} \tag{15}$$

$$\text{where:} \qquad g\left(\frac{|\mathbf{Y}-\mathbf{Y}'|^2}{2}\right) = \frac{f(|\mathbf{Y}-\mathbf{Y}'|)}{|\mathbf{Y}-\mathbf{Y}'|}$$

$$= \beta - \frac{K'(|\mathbf{Y}-\mathbf{Y}'|)}{|\mathbf{Y}-\mathbf{Y}'|}. \tag{16}$$

Von Brecht et al.[35] also consider perturbations of $\mathcal{S}^{d-1}$, and get a scalar eigenvalue problem for the linear stability. In this paper, we apply the technique to the kernel in (13) to derive the necessary and sufficient conditions for the collapsing $\mathcal{S}^{d-1}$ to be linearly stable. In what follows, we first describe the general settings of the eigenvalue problem as written in Ref. 35, and then we derive the conditions for stability.

We begin by writing the unit sphere as: $B(\boldsymbol{\xi})\mathbf{e_1}$, where B serves as a rotation matrix, $\mathbf{e_1}$ is a unit vector $(1, 0, \ldots, 0)$ in $\mathbb{R}^d$, and $\boldsymbol{\xi}$ is a parameterization of the unit sphere. The columns of the matrix $B = [\mathbf{b_1}, \mathbf{b_2}, \ldots, \mathbf{b_d}]$ can be defined as the following: $\mathbf{b_1}$ is the position on the sphere, $\hat{\mathbf{b}}_\mathbf{j} = \mathbf{b}_{1\xi_{j-1}}$, the derivative of $\mathbf{b_1}$ with respect to ξ_{j-1}, and $\mathbf{b_j} = \hat{\mathbf{b}}_\mathbf{j}/|\hat{\mathbf{b}}_\mathbf{j}|$ for $2 \leq j \leq d$. The perturbed solution can be written as

$$\mathbf{Y}(\boldsymbol{\xi}) = B(\boldsymbol{\xi}) \cdot (R\mathbf{e_1} + \boldsymbol{\delta}(\boldsymbol{\xi})e^{\lambda t}), \tag{17}$$

$$\boldsymbol{\delta}(\boldsymbol{\xi}) = \epsilon[c_1 S^m(\boldsymbol{\xi}), c_2 \frac{S^m_{\xi_1}(\boldsymbol{\xi})}{|\hat{b}_1|}, \cdots, c_2 \frac{S^m_{\xi_{d-1}}(\boldsymbol{\xi})}{|\hat{b}_{d-1}|}], \tag{18}$$

where R satisfies the radius condition:

$$\int_{-1}^1 g(R^2(1-s))(1-s)(1-s^2)^{\frac{d-3}{2}}\mathrm{d}s = 0, \tag{19}$$

and S^m is a spherical harmonic of mode m. Through the definition of B, we notice that c_1 corresponds to the perturbation in the normal direction and c_2 corresponds to the perturbation in the tangential direction of the shell. Because of the spherical symmetry of the shell, all tangential directions are equivalent.

The linearization of the system (15) and (16) can be formulated as a scalar eigenvalue problem:[35]

$$\lambda \begin{bmatrix} c_1 \\ c_2 \end{bmatrix} = M_d(m) \begin{bmatrix} c_1 \\ c_2 \end{bmatrix}$$

$$= \begin{bmatrix} \alpha + \lambda_{d,m}(g_1) & m(d+m-2)\lambda_{d,m}(g_2) \\ \lambda_{d,m}(g_2) & m(d+m-2)\lambda_{d,m}(g_3)/R^2 \end{bmatrix} \begin{bmatrix} c_1 \\ c_2 \end{bmatrix}, \tag{20}$$

$$\text{with } \alpha = vol(\mathcal{S}^{d-2})\int_{-1}^1 (1-s^2)^{\frac{d-3}{2}} \cdot$$

$$\left(g(R^2(1-s)) + R^2 g'(R^2(1-s))(1-s)^2\right)\mathrm{d}s,$$

$$g_1(s) = R^2 g'(R^2(1-s))(1-s)^2 - g(R^2(1-s))s,$$

$$g_2(s) = g(R^2(1-s))(1-s),$$

$$g_3'(s) = -R^2 g(R^2(1-s)). \tag{21}$$

Here, m denotes the mode of the spherical harmonic and, for any function h smooth enough,

$$\lambda_{d,m}(h) = vol(\mathcal{S}^{d-2})\int_{-1}^1 h(s)P_m^{(d/2-1)}(s)(1-s^2)^{\frac{d-3}{2}}\mathrm{d}s, \tag{22}$$

where $P_m^{(d/2-1)}$ are Gegenbauer polynomials,[39] normalized so that $P_m(1) = 1$.

TABLE I. Summary of the stability of $\mathcal{S}^{d-1}$ with respect to the power γ and mode m.

$\gamma \backslash m$	$m \geq 2$ and even	$m \geq 2$ and odd
$\gamma \in (2, 2m - 2)$ and $0.5 < \gamma/4 - [\gamma/4] < 1$	stable	stable
$\gamma \in (2, 2m - 2)$ and $0 < \gamma/4 - [\gamma/4] < 0.5$	unstable	unstable
$\gamma \in (2, 2m - 2)$ and $\gamma/4 - [\gamma/4] \in \{0, 0.5\}$	neutrally stable	neutrally stable
$\gamma > 2m - 2$	stable	unstable

We observe that g_1, g_2, and g_3 are essentially polynomials of $1 - s$, for which we have the following formula:

$$\lambda_{d,m}((1-s)^p)$$
$$=(-1)^m 2^{p+d-2} \frac{vol(\mathcal{S}^{d-2})\Gamma(p+\frac{d-1}{2})\Gamma(p+1)\Gamma(\frac{d-1}{2})}{\Gamma(m+p+d-1)\Gamma(1-m+p)}. \tag{23}$$

The necessary and sufficient condition for the system to be stable with mode m perturbation is that the matrix $M_d(m)$ is negative definite – that is, the trace being negative and determinant being positive. Using (23), we obtain the following two conditions for stability of mode m perturbation for (15) and (16):

(i) $\lambda_{d,m}((1-s)^{\frac{\gamma}{2}}) < 0,$

(ii) $\alpha + (2R^2)^{\frac{\gamma-2}{2}}\lambda_{d,m}((1-s)^{\frac{\gamma-2}{2}})$

$$< \frac{2-\gamma}{2}\lambda_{d,m}((1-s)^{\frac{\gamma}{2}}). \tag{24}$$

By applying the identity (23), condition (i) in (24) can be simplified to:

$$\frac{(-1)^m}{\Gamma(1-m+\frac{\gamma}{2})} < 0. \tag{25}$$

One can also show that condition (ii) in (24) is always satisfied for $d \geq 2$ and $m \geq 2$, as it is equivalent to the following inequality:

$$(3 - \gamma - \frac{d-1}{\gamma+d-3}) + \frac{(-1)^{m+1}\Gamma(\frac{\gamma}{2}+d-1)\Gamma(\frac{\gamma}{2}+1)}{\Gamma(m+\frac{\gamma}{2}+d-1)\Gamma(1-m+\frac{\gamma}{2})}$$
$$\times (\gamma - 2 - \frac{(m+\frac{\gamma}{2}+d-2)(\frac{\gamma}{2}-m)}{(\frac{\gamma}{2}+\frac{d-3}{2})\frac{\gamma}{2}}) < 0, \tag{26}$$

which we prove in the Appendix. We first note that the only factor which now determines the stability is (25). Notice also that (25) is independent of the dimension d. The stability conditions are summarized in Table I. Interestingly, all the modes are stable for $2 < \gamma \leq 4$, indicating the linear stability of the shell solution; $m = 3$ gives the unstable mode for all $\gamma > 4$, indicating the linear instability of the shell solution.

B. Particle simulations on shell stability

In this subsection, we investigate the different regimes of (in-)stability in $\mathbb{R}^2$ as predicted from Table I to see how they manifest themselves in the nonlinear dynamics. To do so we apply a fourth
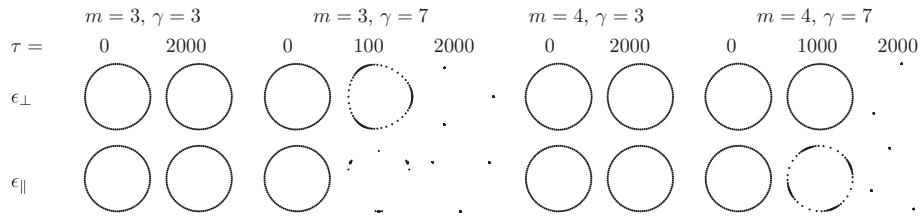
FIG. 1. Simulations of (12) and (27) with various m and γ. The $\epsilon_\perp$ on the first row indicates that $\epsilon_\parallel = 0$ and $\epsilon_\perp = r_0/100$ for initial condition; the $\epsilon_\parallel$ on the second row indicates that $\epsilon_\perp = 0$ and $\epsilon_\parallel = r_0/100$ for initial condition. We use $N = 100$ particles to perform the simulation and these structures have varying radii from 0.35 to 0.6.

order Runge Kutta Method to (12) in $\mathbb{R}^2$ and (13) with initial condition

$$\mathbf{Y}_k = R \begin{pmatrix} \cos \frac{2\pi k}{N} \\ \sin \frac{2\pi k}{N} \end{pmatrix} + \epsilon_\perp \cos \frac{2\pi mk}{N} \begin{pmatrix} \cos \frac{2\pi k}{N} \\ \sin \frac{2\pi k}{N} \end{pmatrix}$$

$$+ \epsilon_\parallel \sin \frac{2\pi mk}{N} \begin{pmatrix} -\sin \frac{2\pi k}{N} \\ \cos \frac{2\pi k}{N} \end{pmatrix}, \tag{27}$$

where $k \in \{1, 2, \ldots, N\}$, and R satisfies the radius condition (19). $\epsilon_\perp$ represents the magnitude of the perturbation in the normal direction to the circle and $\epsilon_\parallel$ represents the magnitude of the perturbation in the tangential direction to the circle.

The simulations for eight cases are plotted in Figure 1. The ring solutions under $m = 3$, $\gamma = 3$ and $m = 4$, $\gamma = 3$ are linearly stable, and the fully nonlinear dynamics are consistent with this. The ring solution under $m = 3$, $\gamma = 7$, and $m = 4$, $\gamma = 5$ deforms to three or four clusters as predicted by Table I. However, the ring solution under normal perturbation deforms much slower than under tangential perturbation, as is shown for $m = 3$ and $\gamma = 7$. Moreover, in the case $m = 4$, $\gamma = 5$, the mode 4 normal perturbation is stable while mode 4 tangential perturbation is unstable, and the mode 3 perturbation comes in through roundoff error and develops into three clusters.

In Figure 2, we plot the time evolution of (12) and (27) with $m = 5$, $\gamma = 40$ and $m = 7$, $\gamma = 40$. We observe that the modes 5 and 7 instabilities grow and develop into clusters. However, in both cases the long time dynamics result in a final ground state of clusters of 3. This can be understood from the linear theory which predicts that the mode 3 eigenvalue is much larger than those corresponding to modes 5 and 7 in the case of γ close to 4, however for larger γ these eigenvalues become comparable. $\gamma = 40$ guarantees that the eigenvalues for mode 5 and 7 are comparable to that of mode 3 and thus we see transient mode 5 and mode 7 behavior until the transition to the final ground state of a 3 cluster. In Sec. IV, we will study the cluster stability of various clusters and we will see that even though Table I tells us that 5 and 7 perturbations of the ring solution are both unstable for $\gamma > 12$, (38) predicts 5 and 7 clusters to be unstable, and 3 clusters are stable for $\gamma > 6$.
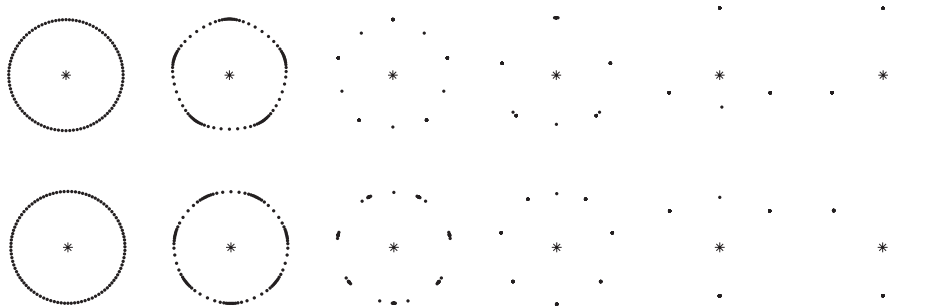

FIG. 2. Simulations for time evolution of (12) and (27) with $N = 100$ particles for $m = 5$ *(first row)* and $m = 7$ *(second row)*, and $\gamma = 40$. The initial perturbation is tangential with $\epsilon_\parallel = r_0/100$. The $*$'s are the centers of mass.
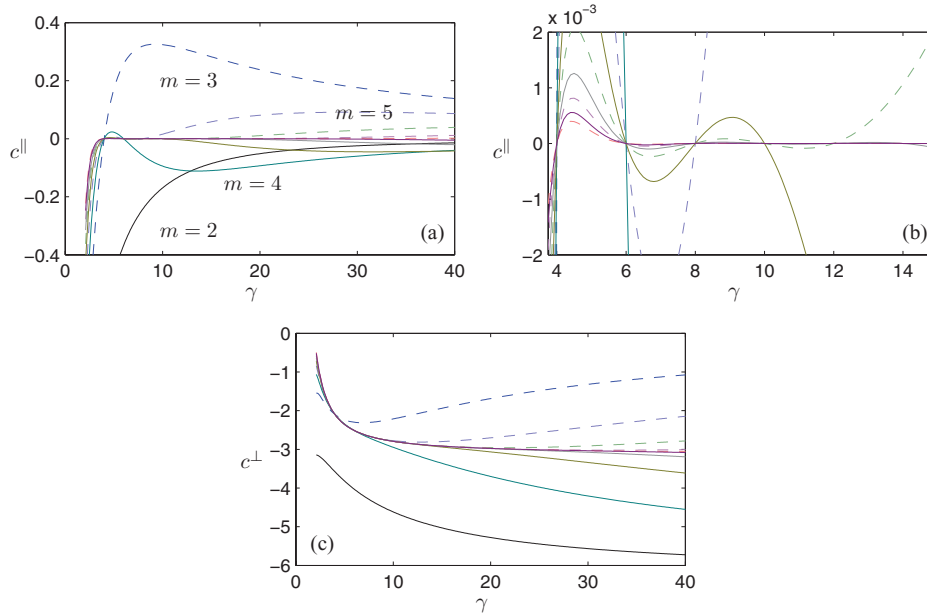
FIG. 3. The eigenvalues of matrix $M(m)$ given by (20) and (21), with respect to different modes m. This plot is for two space dimensions, but for general space dimensions the behavior has the same qualitative features. The solid curves are for m even; while the dashed curves are for m odd. (a) The larger eigenvalue of the two; (b) an enlargement of a long and thin region in (a); (c) the smaller eigenvalue of the two.

Simulations of (12) and (27) capture the predicted instabilities of the collapsing ring solutions from the linear theory. We have also simulated the original time dependent equations

$$\dot{\mathbf{x}}_j = -\sum_k K'(|\mathbf{x}_j - \mathbf{x}_k|)\frac{\mathbf{x}_j - \mathbf{x}_k}{|\mathbf{x}_j - \mathbf{x}_k|}m_k, \tag{28}$$

which is a discrete analogue of (3) and (4), with the initial condition given by (27) for varying values of m and γ. The results are consistent with the simulations of (12) and (27). However, the restriction of machine precision does not allow the simulations to go too far in time. The simulations are not trustworthy when the collapsing ring approaches the roundoff error.

The stability of all the mode m perturbations of $\mathcal{S}^{d-1}$ as indicated by Table I agrees exactly with the calculation of $M(m)$ given by (20) and (21) for modes 2 to 10 for $2 < \gamma \leq 20$. We more closely investigate the eigenvalues (and hence stability) dependence on γ in Figure 3. In Figure 3(a) we plot the bigger of the two eigenvalues, which generally corresponds to tangential perturbations; in Figure 3(b) we plot the smaller of the two eigenvalues, and mainly corresponds to the radial perturbations; and in Figure 3(c) we have enlarged a thin and long region in Figure 3(a) that exhibits the oscillating pattern of the behavior of the bigger eigenvalues with respect to parameter γ.

In Figures 1 and 2, we see cases when $\mathcal{S}^{d-1}$ is unstable and in each of these examples, $\mathcal{S}^{d-1}$ breaks up and collapses to clusters of points. In $\mathbb{R}^2$, the most commonly observed long time attractor is a three point cluster that are 3 vertices of an equilateral triangle. In higher dimensions this behavior continues, i.e., in $\mathbb{R}^3$ the generic attractor is a four point cluster that forms the vertices of a tetrahedron. In Sec. IV, we explain why we observe these attractors by studying the stability of these cluster solutions.

IV. CLUSTER STABILITY

We have now observed when $\mathcal{S}^1$ is linearly unstable it generically breaks up into evenly distributed clusters of particles. In two dimensions the distribution of these clusters is very often an equilateral triangle (again with approximately even numbers of points at each vertex) and in this

section we explain why this shape is the general attractor for the destabilized $\mathcal{S}^1$. We then leverage these results in $\mathbb{R}^2$ to understand the clustering behavior in $\mathcal{S}^{d-1}$.

In this study of cluster stability we will restrict ourselves to the case when we have evenly distributed particles among the clusters. We remark that clustering behavior in $\mathbb{R}^2$ has also been studied by another group[40] for a different but related problem. In this section we will consider the clusters in $\mathbb{R}^d$ for both $d = 2$ and $d > 2$. Given n particles in $\mathbb{R}^d$, m clusters may form under a given interaction force f when we impose the condition that $\frac{n}{m} \in \mathbb{N}$. Let us denote the cluster configuration as $\{\mathbf{p}_{d,1}, \mathbf{p}_{d,2}, \ldots, \mathbf{p}_{d,m}\}$, and order the particles gathering in the ith cluster $\mathbf{p}_{d,i}$ as $\mathbf{Y}_{i,j}$, with $j \in \{1, 2, \ldots, \frac{n}{m}\}$. In two dimensions, the positions of the clusters $\mathbf{p}_{2,i}$ will be equally distributed on the ring (see the statement of Theorem 4.1). Thus for our stability analysis we consider perturbations $\boldsymbol{\epsilon}_{i,j}$ on each particle such that $\mathbf{Y}_{i,j}$, so that $\mathbf{Y}_{i,j} = \mathbf{p}_{i,j} + \boldsymbol{\epsilon}_{i,j}$.

A. Stability of clusters in $\mathbb{R}^2$

We begin by summarizing in Theorem 4.1 the stability of clusters in $\mathbb{R}^2$ for a general interaction kernel, f, which we then prove in the remainder of this section.

Theorem 4.1: *Consider the discrete cluster problem* (12) *in $\mathbb{R}^2$ and let r satisfy the radius condition*

$$\sum_{k=1}^{m} f(2r \sin \frac{\pi k}{m}) \sin \frac{\pi k}{m} = 0, \tag{29}$$

then the m cluster configuration $\mathbf{p}_{2,k} = \left(r \cos \frac{2\pi k}{m}, r \sin \frac{2\pi k}{m}\right)$ with $\frac{n}{m} \in \mathbb{Z}$ particles in each cluster is stable if and only if the following two conditions are satisfied:

1. $c^\perp \leq 0$ *and* $c^\parallel \leq 0$, *with $c^\perp$ and $c^\parallel$ defined below in* (30).

$$
c^\perp = \frac{1}{m} \sum_{k'=1}^{m} \left(\left(\frac{f'(2r \sin \frac{\pi k'}{m})}{2} + \frac{f(2r \sin \frac{\pi k'}{m})}{4r \sin \frac{\pi k'}{m}} \right) \right.
$$
$$
\left. - \left(\frac{f'(2r \sin \frac{\pi k'}{m})}{2} - \frac{f(2r \sin \frac{\pi k'}{m})}{4r \sin \frac{\pi k'}{m}} \right) \cos \frac{2\pi k'}{m} \right),
$$
$$
c^\parallel = \frac{1}{m} \sum_{k'=1}^{m} \left(\left(\frac{f'(2r \sin \frac{\pi k'}{m})}{2} + \frac{f(2r \sin \frac{\pi k'}{m})}{4r \sin \frac{\pi k'}{m}} \right) \right.
$$
$$
\left. + \left(\frac{f'(2r \sin \frac{\pi k'}{m})}{2} - \frac{f(2r \sin \frac{\pi k'}{m})}{4r \sin \frac{\pi k'}{m}} \right) \cos \frac{2\pi k'}{m} \right). \tag{30}
$$

2. *The matrix $A(l)$ with entries $A_{11}(l)$, $A_{12}(l)$, $A_{21}(l)$, $A_{22}(l)$ defined below in* (31) *is non-positive definite for $l \in \{0, 1, 2, \ldots, \left[\frac{m-1}{2}\right]\}$.*

$$A_{11}(l) = A_{22}(-l)$$
$$
= \frac{1}{m} \sum_{k'=1}^{m} \left(\frac{f'(2r \sin \frac{\pi k'}{m})}{2} + \frac{f(2r \sin \frac{\pi k'}{m})}{4r \sin \frac{\pi k'}{m}} \right) \left(1 - \cos \frac{2\pi k'(l+1)}{m}\right),
$$
$$A_{12}(l) = A_{21}(l)$$
$$
= \frac{1}{m} \sum_{k'=1}^{m} \left(-\frac{f'(2r \sin \frac{\pi k'}{m})}{2} + \frac{f(2r \sin \frac{\pi k'}{m})}{4r \sin \frac{\pi k'}{m}} \right) \left(\cos \frac{2\pi k'}{m} - \cos \frac{2\pi k'l}{m} \right). \tag{31}
$$

We prove this by classifying the cluster instabilities that may occur into two types. The first kind of instability comes from fixing the center of mass for each cluster. Since each particle has two

principle directions of freedom, the tangential and radial directions, and fixing the center of mass in both directions reduces two degrees of freedom for each cluster, the total degrees of freedom for the first kind of instability is $2(n - m)$. The second kind of instability comes in by considering the stability of centers of mass for the clusters by regarding each cluster as a single particle, introducing another $2m$ degrees of freedom which brings the total degrees of freedom to $2n$ which is the dimension of the problem. We will classify the stability of each of these types of instabilities to prove Theorem 4.1.

Proof: Let $\epsilon_{k,j}^{\perp}$ represent the normal perturbation, and $\epsilon_{k,j}^{\parallel}$ represent the tangential perturbation of $\mathbf{Y}_{k,j}$, then we can write:

$$\mathbf{Y}_{k,j} = \begin{bmatrix} \cos \frac{2\pi k}{m} & -\sin \frac{2\pi k}{m} \\ \sin \frac{2\pi k}{m} & \cos \frac{2\pi k}{m} \end{bmatrix} \cdot \begin{bmatrix} r + \epsilon_{k,j}^{\perp} \\ \epsilon_{k,j}^{\parallel} \end{bmatrix}, \tag{32}$$

where k is the index of clusters, j is the index of particles in each cluster, while r satisfies the discrete radius condition (29).

First, we assume that the center of mass of each cluster is fixed, i.e., $\sum_j \epsilon_{k,j}^{\perp} = 0$ and $\sum_j \epsilon_{k,j}^{\parallel} = 0$ $\forall\, k \in \{1, 2, \ldots, m\}$. The Taylor expansion of (12) yields to leading order

$$\dot{\epsilon}_{k,j}^{\perp} = c^{\perp} \epsilon_{k,j}^{\perp} \qquad \dot{\epsilon}_{k,j}^{\parallel} = c^{\parallel} \epsilon_{k,j}^{\parallel} \tag{33}$$

with $c^{\perp}$ and $c^{\parallel}$ defined in (30). This means that all the $2(n - m)$ degrees of freedom are fully decoupled and hence independent of each other. Thus, positivity of $c^{\parallel}$ or $c^{\perp}$ determines, respectively, the tangential or radial instabilities.

We next consider the second kind of instability where the center of mass for the particles in each cluster experiences a perturbation. There are $2m$ degrees of freedom associated with this type of perturbation. Since the system is finite dimensional, it suffices to do an explicit calculation of linear stability. Let us now consider the following configuration:

$$\mathbf{p}_{2,k} = \begin{bmatrix} \cos \frac{2\pi k}{m} & -\sin \frac{2\pi k}{m} \\ \sin \frac{2\pi k}{m} & \cos \frac{2\pi k}{m} \end{bmatrix} \cdot \left(\begin{bmatrix} r \\ 0 \end{bmatrix} + \begin{bmatrix} \epsilon_k^{\perp} \\ \epsilon_k^{\parallel} \end{bmatrix} \right), \tag{34}$$

with r satisfying (29) and

$$\begin{bmatrix} \epsilon_k^{\perp} \\ \epsilon_k^{\parallel} \end{bmatrix} = \sum_{l=0}^{m-1} \left(\phi_l \begin{bmatrix} \cos \frac{2\pi kl}{m} \\ \sin \frac{2\pi kl}{m} \end{bmatrix} + \psi_l \begin{bmatrix} \sin \frac{2\pi kl}{m} \\ \cos \frac{2\pi kl}{m} \end{bmatrix} \right), \tag{35}$$

where $\phi_m := \phi_0$ and $\psi_m := \psi_0$. Taylor expansions again lead us to the following eigenvalue problem:

$$\begin{bmatrix} \dot{\phi}_l \\ \dot{\phi}_{m-l} \end{bmatrix} = \begin{bmatrix} A_{11}(l) & A_{12}(l) \\ A_{21}(l) & A_{22}(l) \end{bmatrix} \cdot \begin{bmatrix} \phi_l \\ \phi_{m-l} \end{bmatrix},$$

$$\begin{bmatrix} \dot{\psi}_l \\ \dot{\psi}_{m-l} \end{bmatrix} = \begin{bmatrix} A_{11}(l) & -A_{12}(l) \\ -A_{21}(l) & A_{22}(l) \end{bmatrix} \cdot \begin{bmatrix} \psi_l \\ \psi_{m-l} \end{bmatrix}, \tag{36}$$

with $l \in \{0, 1, 2, \ldots \left[\frac{m-1}{2}\right]\}$, where $A_{11}(l), A_{12}(l), A_{21}(l), A_{22}(l)$ are defined in (31). Thus, the second kind of stability is equivalent to $A(l)$ being non-positive definite with $l \in \{0, 1, 2, \ldots \left[\frac{m-1}{2}\right]\}$. This completes the proof of Theorem 4.1. $\square$

Remark: The two-dimensional linear systems in (36) reduce to one dimension in certain cases. For the case $l = \frac{m}{2}$ with m even or $l = 0$, we have $l = m - l$ and hence $\phi_l = \phi_{m-l}$, $\psi_l = \psi_{m-l}$. Furthermore, we have $A_{11}(l) = A_{22}(l)$ and $A_{12}(l) = A_{21}(l)$. Hence (36) becomes $\dot{\phi}_l = (A_{11}(l) + A_{12}(l))\phi_l$ and $\dot{\psi}_l = (A_{11}(l) - A_{12}(l))\psi_l$, and the condition that $A_{11}(l) + A_{12}(l) \leq 0$ and $A_{11}(l) - A_{12}(l) \leq 0$ is equivalent to $A(l)$ being non-positive definite. When $l = 0$, it is a direct verification that $A_{11}(l) + A_{12}(l) < 0$ and $A_{11}(l) - A_{12}(l) = 0$, corresponding to our intuition that the expansion is stable and rotation is neutrally stable.

By plugging in our specific kernel f defined in (13) to (30) and (31), we arrive at:

$$c^\perp = \frac{1}{m} \sum_{k'=1}^{m} \left(\beta - \frac{\gamma}{2}(2r \sin \frac{\pi k'}{m})^{\gamma-2} \right.$$

$$\left. + \frac{\gamma-2}{2}(2r \sin \frac{\pi k'}{m})^{\gamma-2} \cos \frac{2\pi k'}{m} \right),$$

$$c^\parallel = \frac{1}{m} \sum_{k'=1}^{m} \left(\beta - \frac{\gamma}{2}(2r \sin \frac{\pi k'}{m})^{\gamma-2} \right.$$

$$\left. - \frac{\gamma-2}{2}(2r \sin \frac{\pi k'}{m})^{\gamma-2} \cos \frac{2\pi k'}{m} \right). \tag{37}$$

$$
\begin{cases}
A_{1,1} = \frac{1}{\gamma-2} - \frac{\gamma}{2(\gamma-2)} \frac{\sum_{j=0}^{m-1} \sin^{\gamma-2} \frac{\pi j}{m} \sin^2 \frac{\pi j(l+1)}{m}}{\sum_{j=0}^{m-1} \sin^\gamma \frac{\pi j}{m}}, \\[6pt]
A_{1,2} = A_{2,1} = -\frac{1}{2} + \frac{1}{2} \frac{\sum_{j=0}^{m-1} \sin^{\gamma-2} \frac{\pi j}{m} \sin^2 \frac{\pi jl}{m}}{\sum_{j=0}^{m-1} \sin^\gamma \frac{\pi j}{m}}, \\[6pt]
A_{2,2} = \frac{1}{\gamma-2} - \frac{\gamma}{2(\gamma-2)} \frac{\sum_{j=0}^{m-1} \sin^{\gamma-2} \frac{\pi j}{m} \sin^2 \frac{\pi j(l-1)}{m}}{\sum_{j=0}^{m-1} \sin^\gamma \frac{\pi j}{m}}, \\[6pt]
\qquad\qquad \text{if } l \in \{0, \ldots, \left[\frac{m}{2}\right]\} \text{ and } l \neq 1 \\[6pt]
A_{1,1} = \frac{1-2\gamma}{\gamma-2} + \frac{2\gamma}{\gamma-2} \frac{\sum_{j=0}^{m-1} \sin^{\gamma+2} \frac{\pi j}{m}}{\sum_{j=0}^{m-1} \sin^\gamma \frac{\pi j}{m}}, \\[6pt]
A_{1,2} = A_{2,1} = A_{2,2} = 0 \\[6pt]
\qquad\qquad \text{if } l = 1.
\end{cases} \tag{38}
$$

Equations (37) and (38) complete the clusters stability in $\mathbb{R}^2$ for f. However, since there is no closed form of $\sum_{k'=1}^{m-1} \sin^\gamma \frac{\pi k'}{m}$ for general $\gamma > 2$, we cannot evaluate them analytically. Therefore we numerically investigate Eqs. (37) and (38) in Sec. IV B.

B. Numerical simulations of cluster stability in $\mathbb{R}^2$

Figure 4 contains plots of (37) for various values of m. From the plot, we see that the tangential stability of clusters exactly complements the stability of $\mathcal{S}^1$ as indicated in Figure 3 and Table I. By comparing the stability summary Table I for $\mathcal{S}^1$ with the summary Table III for cluster stability we see that, precisely when the ring is unstable ($\gamma > 4$), there is at least one cluster that is stable; yet when the ring is stable no cluster is stable.

Moreover when we look in Figure 2 (which is the large γ regime) we see the 5 and 7 clusters eventually relax to the equilateral 3 cluster on longer timescales. This is understood because the 5 and 7 clusters are saddle points which have many decaying directions but just one or two growing directions. These eventually break up into a stable 3 cluster. The growing directions can be computed in the stability analysis of the clusters with moving center of mass, as summarized in (38).

We summarize the second kind of instability (center of mass) in Table II by simulating Eq. (38) for $l \in \{0, 1, \ldots, \left[\frac{m}{2}\right]\}$. By combining the results in Figure 4 and Table II, we obtain Table III for the complete cluster stability in $\mathbb{R}^2$.

We also perform simulations of (12) with initial condition (32), where r satisfies the radius condition (29), and $\epsilon_{k,j}^\parallel$ and $\epsilon_{k,j}^\perp$ are small randomly chosen perturbations. As we can see from Figure 5, for $\gamma < 4$, the clusters solution for any m is unstable and eventually expands to a circle, but for $\gamma > 4$, m clusters always deform to 3 clusters, except for some cases when $4 < \gamma < 6$ with $m \in \{4, 5\}$ which agrees precisely with Table III.
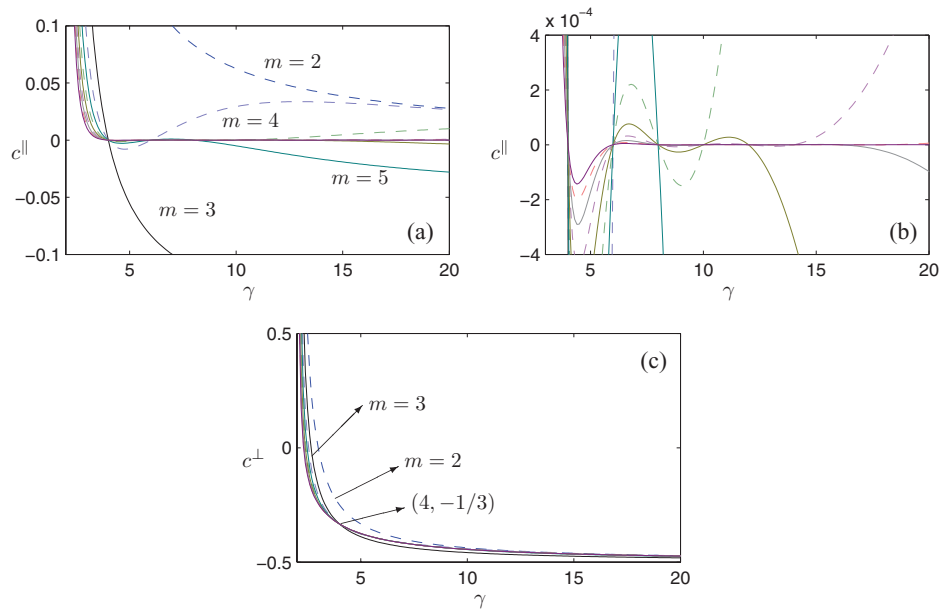
FIG. 4. We plot the behavior of $c^\perp$ and $c^\parallel$ in (37) for various values of m. The dashed curves are for m even, while the solid ones are for m odd. (a) The tangential eigenvalues $c^\parallel$ in (37); (b) an enlargement along the the γ-axis of (a); (c) the normal eigenvalues $c^\perp$ in (37). In (c), all the curves except $m = 2$ intersect at $\gamma = 4$ with value $c^\perp = -1/3$. The curve for $m = 3$ intersects 0 at $\gamma = 8/3$, indicating that mode 3 normal perturbation changes stability at $\gamma = 8/3$.

C. Stability of clusters in general space dimensions

Figure 5 and Table III give the whole picture of cluster stability in $\mathbb{R}^2$ for f defined in (13). However, the argument does not extend naturally to higher dimensions. We observe that when $2 < \gamma < 4$, the clusters are unstable for any m, but for $\gamma > 4$ and $m = 3$, the clusters are always stable. For $4 < \gamma < 6$, the clusters with $m = 4$ or $m = 5$ are also stable but $m = 3$ is the largest negative and therefore dominant eigenvalue of them (see Figure 4). In fact, from our simulations, the $m = 3$ cluster with equally sized clusters is the global attractor for $\gamma > 4$ for generic initial conditions - though we have only proved that it is a local attractor in this paper. This configuration is in fact the vertices of an equilateral triangle, so we refer to it as such. In general space dimensions $\mathbb{R}^d$, it is a natural guess that the simplex configuration - a higher dimensional generalization of the equilateral triangle - is a local attractor for $\gamma > 4$ in $\mathbb{R}^d$. We prove this result in this section.

Let us define the vertices of a simplex in general space dimension in the following sequential way: We begin by writing the vertices of an equilateral triangle as the following three points:

$$\mathbf{p}_{2,1} = (r, 0), \qquad \mathbf{p}_{2,2} = (r \cos\theta_2, r \sin\theta_2),$$
$$\mathbf{p}_{2,3} = (r \cos\theta_2, -r \sin\theta_2), \tag{39}$$

TABLE II. Stability table for center of mass of clusters, corresponding to the second kind of instability. It is stable if and only if the eigenvalues of $A(l)$ defined by (38) are all nonpositive.

	$m = 3$ or $m = 4$	$m = 5$	$m \geq 6$
$\gamma \in (2, 4]$	stable	stable	stable
$\gamma \in (4, 6]$	stable	stable	unstable
$\gamma \in (6, \infty)$	stable	unstable	unstable

TABLE III. Stability table for m clusters, combining both kinds of instabilities. It is stable if and only if conditions 1 and 2 in Theorem 4.2 are satisfied.

	$m = 3$	$m = 4$ or $m = 5$	$m \geq 6$
$\gamma \in (2, 4]$	unstable	unstable	unstable
$\gamma \in (4, 6]$	stable	stable	unstable
$\gamma \in (6, \infty)$	stable	unstable	unstable

with $\theta_2 = 2\pi/3$. We can naturally express the vertices of a tetrahedron using this notation as the following four points:

$$\mathbf{p}_{3,1} = (r, 0, 0), \quad \mathbf{p}_{3,2} = (r \cos\theta_3, \sin\theta_3 \mathbf{p}_{2,1}),$$

$$\mathbf{p}_{3,3} = (r \cos\theta_3, \sin\theta_3 \mathbf{p}_{2,2}), \quad \mathbf{p}_{3,4} = (r \cos\theta_3, \sin\theta_3 \mathbf{p}_{2,3}), \tag{40}$$

with $\theta_3 = \arccos(-\frac{1}{3})$. Let us call the vertices of an equilateral triangle $\mathbf{p}_2 := \{\mathbf{p}_{2,1}, \mathbf{p}_{2,2}, \mathbf{p}_{2,3}\}$ a simplex in $\mathbb{R}^2$, and the vertices of a regular tetrahedron $\mathbf{p}_3 := \{\mathbf{p}_{3,1}, \mathbf{p}_{3,2}, \mathbf{p}_{3,3}, \mathbf{p}_{3,4}\}$ the vertices of a simplex in $\mathbb{R}^3$. In higher dimensions we have the following recursive relation for $\mathbf{p}_{i,j}$:

$$\mathbf{p}_{i,1} = (r, 0, \cdots, 0),$$

$$\mathbf{p}_{i,j} = (r \cos(\theta_i), \sin(\theta_i)\mathbf{p}_{i-1,j-1}) \text{ for } j \geq 2, \tag{41}$$

where $\theta_i = \arccos(-\frac{1}{i})$. It is easy to verify that:

$$\frac{\mathbf{p}_{i,j}}{|\mathbf{p}_{i,j}|} \cdot \frac{\mathbf{p}_{i,j'}}{|\mathbf{p}_{i,j'}|} = -\frac{1}{i} \text{ for } j \neq j'. \tag{42}$$

and we set $\mathbf{p}_i := \{\mathbf{p}_{i,1}, \ldots, \mathbf{p}_{i,i+1}\}$ to be the vertices of a simplex in $\mathbb{R}^i$. Notice that for the vertices of a simplex to be a steady state for (12) and (13), we need the distance λ between any two points $\mathbf{p}_{i,j}$ and $\mathbf{p}_{i,j'}$ to be exactly the zero of f in (13). We summarize this discussion in the following definition.

Definition. A simplex configuration solution is a configuration with clusters $\{\mathbf{p}_{d,1}, \mathbf{p}_{d,2}, \ldots, \mathbf{p}_{d,d+1}\}$ as vertices of a simplex with inter-vertex distance $\lambda > 0$ where $f(\lambda) = 0$. We also enforce that at each cluster $\mathbf{p}_{d,i}$ there are an equal number particles $\{\mathbf{Y}_{i,j}, j \in \{1, 2, \ldots, \frac{n}{m}\}\}$.

Given this definition we can now write our perturbation ansatz of our simplex solution as:

$$\epsilon_{i,j} = \mathbf{Y}_{i,j} - \mathbf{p}_{d,i}.$$

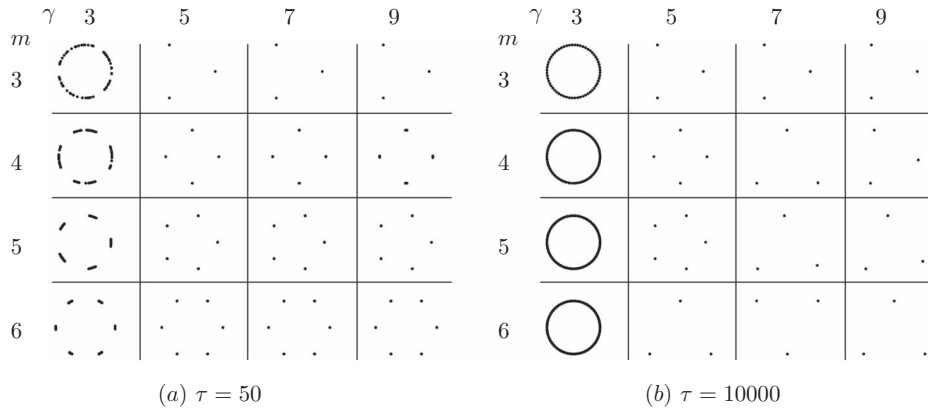(a) $\tau = 50$ (b) $\tau = 10000$

FIG. 5. Numerical simulation of the m clusters problem, with $m = 3, 4, 5, 6$ and $\gamma = 3, 5, 7,$ and 9, each hole starting with $n = 20$ particles with fixed-center small random perturbation. (a) and (b) are the plot of the particles at time $\tau = 50$ and $\tau = 10\,000$, respectively.

We now state our main result which is that it is enough to just study the stability in $\mathbb{R}^2$ to classify the stability of simplex solutions in $\mathbb{R}^d$.

Theorem 4.2: *Consider the cluster problem* (12) *in* $\mathbb{R}^d$, *the simplex configuration solution is a stable configuration if and only if the following two conditions are satisfied:*

1. *The simplex configuration in* $\mathbb{R}^2$ *is stable under tangential perturbations* $\epsilon_{i,j}$ *with* $\sum_j \epsilon_{i,j} = 0$ $\forall i$.
2. $f'(0) + \frac{d+1}{2} f'(\lambda) \leq 0$.

Remark: Recall that f being repulsive at short distance and attractive at long distance implies that there is only one non-zero root of f. For our particular f defined by (13), we have $\lambda = \beta^\beta$, $f'(0) = \beta$, and $f'(\lambda) = -1$, so condition 2 of Theorem 4.2 reads $\gamma \geq 2 + \frac{2}{d-1}$. Thus, the simplex configuration is stable for $\gamma \geq 4$ and unstable for $2 < \gamma < 4$.

To prove the above theorem, we make use of the following three lemmas:

Lemma 4.3: The simplex configuration in $\mathbb{R}^d$, $d > 2$ *is stable under tangential perturbations* $\epsilon_{i,j}$ *of particles* $\mathbf{Y}_{i,j}$ *with* $\sum_j \epsilon_{i,j} = 0 \ \forall \ i \iff$ *the simplex configuration in* $\mathbb{R}^2$ *under tangential perturbations of each particle* $\mathbf{Y}_{i,j}$ *with* $\sum_j \epsilon_{i,j} = 0 \ \forall \ i$.

Lemma 4.4: The simplex configuration in $\mathbb{R}^d$ *is stable under normal perturbations of particles* $\mathbf{Y}_{i,j}$ *with* $\sum_j \epsilon_{i,j} = 0 \ \forall i \iff 2f'(0) + (d + 1)f'(\lambda) \leq 0$.

Lemma 4.5: The simplex configuration in $\mathbb{R}^d$ *is always stable under perturbations to the positions of each cluster* $\mathbf{p}_{d,j}$.

We first provide a short proof of Theorem 4.2 and then prove Lemmas 4.3–4.5.

Proof of Theorem 4.2: A general perturbation of the simplex configuration $\mathbf{Y}_{i,j}$ can be decomposed into three parts: The first being tangential perturbations with the center of mass for each cluster fixed, i.e, $\sum_j \epsilon_{i,j} = 0$ or equivalently $\frac{d+1}{n} \sum_j \mathbf{Y}_{i,j} = \mathbf{p}_{d,i}$, which have $(d-1)(n-d-1)$ degrees of freedom; the second being normal perturbations with the center of mass for each cluster fixed, i.e, $\frac{d+1}{n} \sum_j \mathbf{Y}_{i,j} = \mathbf{p}_{d,i}$, which have $n-d-1$ degrees of freedom; and finally the third being perturbations of clusters $\mathbf{p}_{d,i}$, having $d(d+1)$ degrees of freedom. These three kinds of perturbations are orthogonal to one another and exhaust all the nd degrees of freedom. The third kind of perturbation always decays because of Lemma 4.5 and the first and second kinds of perturbations are considered in Lemmas 4.3 and 4.4, which give the necessary and sufficient conditions for the simplex configuration to be stable in Theorem 4.2. □

Proof of Lemma 4.3: To prove that the tangential perturbations of the simplex configuration in $\mathbb{R}^2$ with $\sum_j \epsilon_{i,j} = 0 \ \forall \ i$ are stable $\iff$ the tangential perturbations of the simplex configuration in $\mathbb{R}^d$ with $\sum_j \epsilon_{i,j} = 0 \ \forall \ i$ are stable for any d, it is enough to prove the following induction statement:
$\forall \ d \geq 2$, the tangential perturbations of the simplex configuration in $\mathbb{R}^d$ with $\sum_j \epsilon_{i,j} = 0 \ \forall \ i$ are stable $\iff$ the tangential perturbations of the simplex configuration in $\mathbb{R}^{d+1}$ with $\sum_j \epsilon_{i,j} = 0$ $\forall \ i$ are stable.
For simplicity, we prove the above statement for the base case $d = 2$, as the inductive step follows similarly to this argument. A simplex configuration in $d = 3$, as shown in Figure 6, is constructed by adding to an equilateral triangle configuration $\{\mathbf{p}_{3,2}, \mathbf{p}_{3,3}, \mathbf{p}_{3,4}\}$ a cluster $\mathbf{p}_{3,1}$ (in $d = 2$) whose projection is right on the center of the triangle $\{\mathbf{p}_{3,2}, \mathbf{p}_{3,3}, \mathbf{p}_{3,4}\}$, with the distance between $\mathbf{p}_{3,1}$ and $\mathbf{p}_{3,i}$ being $\lambda \ \forall \ i \in \{2, 3, 4\}$, and then enforcing that the number of particles in each cluster to be $\frac{n}{4} \in \mathbb{R}$. A general tangential perturbation $\{\epsilon_{i,j}, i \in \{1, 2, 3, 4\}, j \in \{1, 2, \ldots, \frac{n}{4}\}\}$ with $\sum_j \epsilon_{i,j} = 0$ can be written as a linear composition of tangential perturbations to the ith cluster $\{\epsilon_{i,j}, j \in \{1, 2, \ldots, \frac{n}{4}\}\}$. So our task is now to consider the stability of perturbations of the ith cluster with $\sum_j \epsilon_{i,j} = 0$ and $\epsilon_{i',j} = 0 \ \forall \ i' \neq i$.
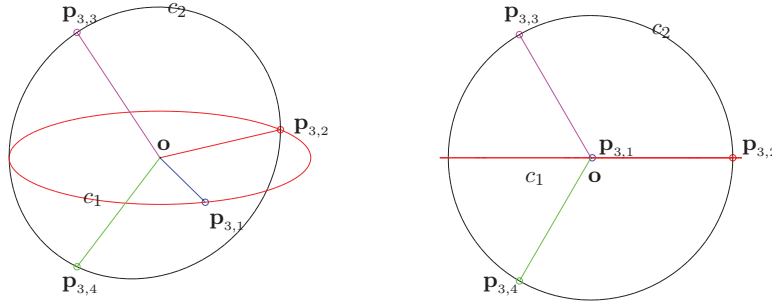
FIG. 6. Regular tetrahedron on sphere.

To classify the stability let us return our attention to Figure 6 and the case $i = 1$ for simplicity. Let us consider the tangential perturbations $\{\boldsymbol{\epsilon}_{1,j}, i \in \{1, 2, \ldots, \frac{n}{4}\}\}$ on the point $\mathbf{p}_{3,1}$, with $\sum \boldsymbol{\epsilon}_{1,j} = 0$. We can further decompose $\boldsymbol{\epsilon}_{1,j}$ uniquely into a tangential component $\boldsymbol{\epsilon}_{1,j}^1$ in the plane determined by three points $\mathbf{p}_{3,1}$, $\mathbf{p}_{3,2}$, $\mathbf{p}_{3,3}$ and a tangential component $\boldsymbol{\epsilon}_{1,j}^2$ in the plane determined by three points $\mathbf{p}_{3,1}$, $\mathbf{p}_{3,3}$, $\mathbf{p}_{3,4}$. The magnitude of the perturbation $\boldsymbol{\epsilon}_{1,j}^1$ satisfies Eq. (33) with $c^{\|}$ determined by (30) and, by Taylor expanding (12), the perturbation $\boldsymbol{\epsilon}_{1,j}^1$ has a higher order therefore negligible effect on particles $\mathbf{Y}_{4,j}$ located at the point $\mathbf{p}_{3,4}$. Thus any perturbation $\{\boldsymbol{\epsilon}_{1,j} = \boldsymbol{\epsilon}_{1,j}^1, \boldsymbol{\epsilon}_{i',j} = 0, \forall i' \neq 1\}$ with arbitrary $\boldsymbol{\epsilon}_{1,j}^1$ and $\sum_j \boldsymbol{\epsilon}_{1,j}^1 = 0$ is an eigenvector of the linearization of (12) with eigenvalue $c^{\|}$. The same analysis applies for $\boldsymbol{\epsilon}_{1,j}^2$. In general, by analyzing perturbations $\{\boldsymbol{\epsilon}_{i,j}, j \in \{1, 2, \ldots, \frac{n}{4}\}\}$ for $i \in \{2, 3, 4\}$ similarly, we find that $\boldsymbol{\epsilon}_{i,j}$ satisfies the following:

$$\dot{\boldsymbol{\epsilon}}_{i,j} = c^{\|}\boldsymbol{\epsilon}_{i,j}, \tag{43}$$

with $c^{\|}$ determined by (30). In another word, any perturbation $\{\boldsymbol{\epsilon}_{i,j}, i \in \{1, 2, 3, 4\}, j \in \{1, 2, \ldots, \frac{n}{4}\}\}$ with $\sum_j \boldsymbol{\epsilon}_{i,j} = 0 \ \forall \ i$ is an eigenvector of the linearization of (33) with eigenvalue $c^{\|}$. The value $c^{\|}$ as calculated for $m = 3$ in $\mathbb{R}^2$ is $f'(0)\frac{f'(\lambda)}{2}$. This completes the base case of $d = 2$.

The induction in higher dimensions is proved similarly by adding a single new point orthogonally to the lower dimensional simplex and then showing that the original simplex has a higher order effect on the tangential linear stability of the new vertex. The details are left to the reader. We can thus conclude that the sign of $f'(0) + \frac{f'(\lambda)}{2}$ determines the stability of tangential perturbations in $\mathbb{R}^d$ with $\sum_j \boldsymbol{\epsilon}_{i,j} = 0$ for all $d \geq 2$. $\qquad \square$

Proof of Lemma 4.4: Consider the simplex configuration $\{\mathbf{p}_{d,i} : i \in \{1, \ldots, d+1\}\}$ in $\mathbb{R}^d$ with $\frac{n}{d+1} \in \mathbb{N}$ particles $\{\mathbf{Y}_{i,j}, j \in \{1, 2, \ldots, \frac{n}{d+1}\}\}$ in each $\mathbf{p}_{d,i}$. Let us now consider perturbations in the normal direction $\boldsymbol{\epsilon}_{i,j} = \epsilon_{i,j}\frac{\mathbf{p}_{d,i}}{|\mathbf{p}_{d,i}|}$ to the point $\mathbf{Y}_{i,j}$. The leading order interaction of particle $\mathbf{Y}_{i',j'}$ from particle $\mathbf{Y}_{i,j}$ is $\frac{1}{n} f'(\lambda)\sqrt{\frac{d+1}{2d}}(\epsilon_{i,j} + \epsilon_{i',j'})\frac{\mathbf{p}_{d,i}-\mathbf{p}_{d,i'}}{|\mathbf{p}_{d,i}-\mathbf{p}_{d,i'}|}$. Under the assumption that $\sum_{j'} \epsilon_{i',j'} = 0$ $\forall \ i'$, we have that by summing over j' the total leading order interaction of particles $\{\mathbf{Y}_{i',j'}, j' \in \{1, 2, \ldots, \frac{n}{d+1}\}\}$ of $\mathbf{p}_{d,i'}$ on particle $\mathbf{Y}_{i,j}$ is $\frac{1}{d+1} f'(\lambda)\sqrt{\frac{d+1}{2d}}\epsilon_{i,j}\frac{\mathbf{p}_{d,i}-\mathbf{p}_{d,i'}}{|\mathbf{p}_{d,i}-\mathbf{p}_{d,i'}|}$. If we now sum over all $i' \neq i$ the total leading order interaction of all the particles $\{\mathbf{Y}_{i',j'}, j' \in \{1, 2, \ldots, \frac{n}{d+1}\}\}$ on the particle $\mathbf{Y}_{i,j}$ as $\frac{1}{2} f'(\lambda)\epsilon_{i,j}\frac{\mathbf{p}_{d,i}}{|\mathbf{p}_{d,i}|}$. We can also easily compute the leading order interaction of all the particles $\{\mathbf{Y}_{i,j'}, j' \in \{1, 2, \ldots, \frac{n}{d+1}\}\}$ in the same cluster $\mathbf{p}_{d,i}$ of particle $\mathbf{Y}_{i,j}$ is $\frac{1}{d+1} f'(0)\epsilon_{i,j}\frac{\mathbf{p}_{d,i}}{|\mathbf{p}_{d,i}|}$. Combing all of the above leading order interactions $\{\mathbf{Y}_{i',j'}, j' \in \{1, 2, \ldots, \frac{n}{d+1}\}\}$ has on $\mathbf{Y}_{i,j}$, we arrive at the following:

$$\dot{\epsilon}_{i,j} = \frac{2f'(0) + (d+1)f'(\lambda)}{2(d+1)}\epsilon_{i,j}. \tag{44}$$

Thus, Lemma 4.4 is proved. $\qquad \square$

For our particular kernel (13), we have $f'(0) = \beta$ and $f'(\beta^\beta) = -1$, hence the normal perturbations with fixed center of mass is stable if and only if $\gamma \geq 2 + \frac{2}{n+1}$.

Proof of Lemma 4.5: We consider perturbations to the center of mass of each cluster $\mathbf{p}_{d,i}$. In this case we need not study the dynamics of each individual particle but instead the interactions between the clusters $\mathbf{p}_{d,i}$. This configuration is analogous to a spring system, with a spring joining each pair $\mathbf{p}_{d,i}$ and $\mathbf{p}_{d,i'}$. Given that f is short range repulsive and long range attractive, each such spring has a spring constant of $-\frac{1}{d+1} f'(\lambda) > 0$, and the spring force of $\mathbf{p}_{d,i'}$ on $\mathbf{p}_{d,i}$ to leading order is $\frac{1}{d+1} f'(\lambda)(|\mathbf{p}_{d,i} - \mathbf{p}_{d,i'}| - \lambda)\frac{\mathbf{p}_{d,i} - \mathbf{p}_{d,i'}}{|\mathbf{p}_{d,i} - \mathbf{p}_{d,i'}|}$. We can therefore define the energy of this system to leading order as

$$E(\mathbf{p}_{d,1}, \mathbf{p}_{d,2}, \ldots, \mathbf{p}_{d,d+1})$$

$$= -\frac{1}{2} \sum_{i' \neq i} \frac{f'(\lambda)}{d+1}(|\mathbf{p}_{d,i} - \mathbf{p}_{d,i'}| - \lambda)^2. \tag{45}$$

It is now straightforward to check that (12) to leading order is a system that describes the gradient flow of the energy as defined by (45). Thus the system settles down to a local minima of E, which is exactly the simplex configuration. □

D. Numerical simulations on simplex configuration

Theorem 4.2 extends the simplex configuration stability in $\mathbb{R}^2$ to arbitrary dimensions which allows us to conclude that for (12) and (13), the simplex configuration in $\mathbb{R}^d$ is unstable for $2 < \gamma < 4$ and stable for $\gamma \geq 4$, for $d \geq 2$.

To observe this phenomena we apply a Range Kutta 45 method to (12) with n randomly selected points $\{\mathbf{Y}_i \in \mathbb{R}^d, i \in \{1, 2, \ldots n\}\}$. After evolving time long enough, the solution approaches final steady state, we measure the normalized inner product of all pairs of two points

$$\left\{\frac{\mathbf{Y}_i}{|\mathbf{Y}_i|} \cdot \frac{\mathbf{Y}_{i'}}{|\mathbf{Y}_{i'}|}, i \neq i'\right\}, \tag{46}$$

and we plot both the final steady state and the probability distribution of the normalized inner products in Figure 7.

It is clear from Figure 7 that for $\gamma = 3$ (in the unstable simplex regime), $\mathcal{S}^{d-1}$ is the stable steady state solution for (12) and (13) while for $\gamma > 5$ (in the stable simplex regime), the simplex solution is the attractor. We also can observe that this behavior is independent of dimension, just as
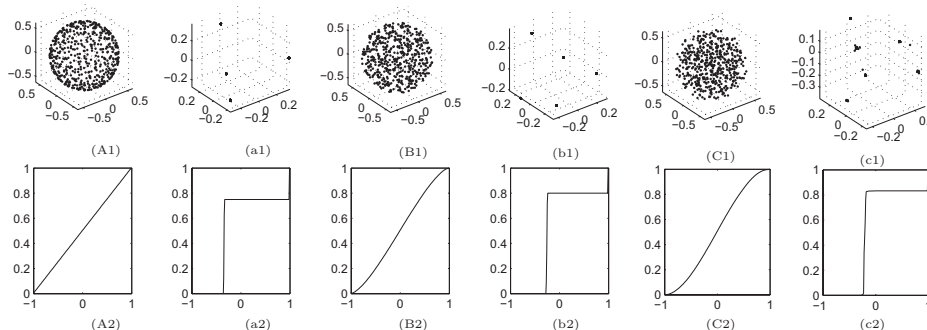

FIG. 7. Numerical simulation of (12) and (13) with $n = 150$ random initial points in $\mathbb{R}^d$. Capital letters correspond to simulations done for $\gamma = 3$ and lower case letters correspond to $\gamma = 5$. **First Row:** Figures (A1) and (a1) are the final computed steady states in $d = 3$. Similarly for (B1), (b1) in $d = 4$ though the plots are projected into $\mathbb{R}^3$ by taking the first three coordinates. (C1) and (c1) are for $d = 5$ and are projections into $\mathbb{R}^3$ by also taking the first three coordinates. **Second Row:** (A2), (a2), (B2), (b2), (C2), and (c2) are plots of the corresponding probability distributions of the normalized inner product of any two points in the final steady state.

we expect. For $\gamma > 5$ in $\mathbb{R}^d$, we have

$$\mathcal{P}\left(\left|\frac{\mathbf{Y}_i}{|\mathbf{Y}_i|} \cdot \frac{\mathbf{Y}_{i'}}{|\mathbf{Y}_{i'}|} + \frac{1}{d}\right| \ll 1\right) \approx \frac{d}{d+1}$$

$$\text{and } \mathcal{P}\left(\left|\frac{\mathbf{Y}_i}{|\mathbf{Y}_i|} \cdot \frac{\mathbf{Y}_{i'}}{|\mathbf{Y}_{i'}|} - 1\right| \ll 1\right) \approx \frac{1}{d+1},$$

indicating that our simulations are close to simplex configurations. We started these simulations with random distributions of particles so these simulations suggest that the simplex configuration may be the global attractor for any $d \geq 2$ and $\gamma \geq 4$.

V. CONCLUSION

In this paper we derive the linear stability of the self-similar collapsing shell solution in the case of a power law interaction potential. In the regime of instability we observe that solutions aggregate to clusters of points, in particular simplex configurations in $\mathbb{R}^d$. We next derive the complimentary stability analysis for these simplex solutions. Taken together, we have a theoretical framework for understanding the dynamics of collapse for this class of problems. For $\gamma > 2$ it was previously shown numerically[1,27] that the collapsing shell profile was the long time attractor when one first restricts to purely radially symmetric solutions. Our analysis shows that for $2 < \gamma < 4$, the shell solution is stable to non-radially symmetric perturbations but for $\gamma > 4$ the shell destabilizes. Our simulations support this analysis and suggest that in the destabilizing regime the solution collapses to clusters of equally distributed points. These clusters are generally in the form of a simplex. We then perform the stability analysis of these simplex distributions and find that the results complement those of the shell. In particular these simplex configurations are unstable precisely when the shell is stable and vice versa.

We have constructed a significant portion of the stability picture of (1) with interaction kernel (2) as a dynamical system. This allows us to predict when collapsing solutions will maintain spherical symmetry or when solutions will aggregate onto more singular simplex configurations. However, the entire story is not complete. *Global* and nonlinear stability of solutions are still open problems. Finally, the cluster problem in arbitrary dimensions with a general (non-simplex) configuration remains open.

ACKNOWLEDGMENTS

APPENDIX: PROOF OF INEQUALITY (26)

In proving the criteria for linear stability of $\mathcal{S}^{d-1}$ in Sec. III A, the inequality (26) is required. We provide a proof of this inequality here. Let us define the following quantity:

$$Q(\gamma, m, d) = \frac{\Gamma(\frac{\gamma}{2} + d - 1)\Gamma(\frac{\gamma}{2} + 1)}{\Gamma(m + \frac{\gamma}{2} + d - 1)\Gamma(1 - m + \frac{\gamma}{2})}. \tag{A1}$$

Then the RHS of Eq. (26) can be written as:

$$(3 - \gamma - \frac{d-1}{\gamma + n - 3}) + (\gamma - 2)(-1)^{m+1}Q(\gamma, m, d)$$

$$+ \frac{\gamma + 2d - 4}{\gamma + d - 3}(-1)^m Q(\gamma - 2, m, d). \tag{A2}$$

The term $Q(\gamma, m, d)$ can be written out as the following:

$$Q(\gamma, m, d) = \frac{\Pi_{i=1}^{m}(\frac{\gamma}{2} - m + i)}{\Pi_{i=1}^{m}(\frac{\gamma}{2} + d - 2 + i)}. \tag{A3}$$

Notice that both $|\frac{\gamma}{2} - m + 1|$ and $\frac{\gamma}{2}$ are less than $\frac{\gamma}{2} + d + m - 2$, so that $|Q(\gamma, m, d)| < 1$ always. Furthermore, if $2 \leq \frac{\gamma}{2} \leq m$ then $|Q(\gamma, m, d)| \leq \frac{1}{\gamma + 2d - 2}$, and $|Q(\gamma - 2, m, d)| \leq \frac{1}{\gamma + 2d - 4}$; while $\frac{\gamma}{2} > m - 1$ implies $0 < Q(\gamma, m, d) < \frac{\gamma - 2m + 2}{\gamma + 2d - 2}$.

We can now assert the inequality (26) by considering the following three cases for $m \geq 2$:

- When $4 \leq \gamma \leq 2m$, we have

$$\begin{aligned}
(A2) &\leq 3 - \gamma - \frac{d - 1}{\gamma + d - 3} + \frac{\gamma - 2}{\gamma + 2d - 2} \\
&\quad + \frac{\gamma + 2n - 4}{\gamma + n - 3} \cdot \frac{1}{\gamma + 2d - 4} \\
&= 4 - \gamma - \frac{d - 2}{\gamma + d - 3} - \frac{2d}{\gamma + 2d - 2} < 0
\end{aligned}$$

- When $\gamma > 2m$, we have

$$\begin{aligned}
(A2) &< 3 - \gamma - \frac{d - 1}{\gamma + d - 3} + (\gamma - 2)\frac{\gamma - 2m + 2}{\gamma + 2d - 2} \\
&\quad + \frac{\gamma - 2m}{\gamma + d - 3}.
\end{aligned}$$

In the case $m \geq 3$, we have

$$\begin{aligned}
(A2) &< -\frac{d - 1}{\gamma + d - 3} - (\gamma - 2)\left(\frac{\gamma - 4}{\gamma - 2} - \frac{\gamma - 2m + 2}{\gamma + 2d - 2}\right) \\
&\quad - \frac{2m + d - 3}{\gamma + d - 3} \\
&\leq -\frac{d - 1}{\gamma + d - 3} - \frac{(\gamma - 2)(\gamma - 2m + 2)(2m + 2d - 6)}{(\gamma - 2m + 4)(\gamma + 2d - 2)} \\
&\quad - \frac{2m + d - 3}{\gamma + d - 3} \\
&< 0;
\end{aligned}$$

while in the case $m = 2$, we have

$$\begin{aligned}
(A2) &< -\frac{2d(\gamma - 2)}{\gamma + 2d - 2} + \frac{2\gamma - 6}{\gamma + d - 3} \\
&\leq -\frac{2d(\gamma - 2)}{\gamma + 2d - 2} + \frac{2\gamma + 2d - 4}{\gamma + 2d - 2} \\
&\leq -\frac{2\left((\gamma - 3)(d - 1) - 1\right)}{\gamma + 2d - 2} < 0
\end{aligned}$$

- When $2 < \gamma < 4$, direct calculations show that we always have $(-1)^{m+1}Q(\gamma, m, d) < 0$ and $(-1)^m Q(\gamma - 2, m, d) < 0$, and it is easy to see that (A2) < 0 in this case.

The above three cases exhaust all the possibilities, and hence we conclude that the inequality (26) holds for $m \geq 2$, $d \geq 2$, and $\gamma \geq 2$.

[1] Y. Huang and A. L. Bertozzi, "Self-similar blowup solutions to an aggregation equation in $\mathbf{R}^n$," SIAM J. Appl. Math. **70**, 2582 (2010).

[2] M. Bodnar and J. J. L. Velazquez, "An integro-differential equation arising as a limit of individual cell-based models," J. Differ. Equations **222**, 341 (2006).

[3] M. Burger, V. Capasso, and D. Morale, "On an aggregation model with long and short range interactions," Nonlinear Anal.: Real World Appl. **8**, 939 (2007).

[4] M. Burger and M. Di Francesco, "Large time behavior of nonlocal aggregation models with nonlinear diffusion," Networks Heterog. Media **3**, 749 (2008).

[5] A. Mogilner and L. Edelstein-Keshet, "A non-local model for a swarm," J. Math. Biol. **38**, 534 (1999).

[6] C. M. Topaz and A. L. Bertozzi, "Swarming patterns in a two-dimensional kinematic model for biological groups," SIAM J. Appl. Math. **65**, 152 (2004).

[7] C. M. Topaz, A. L. Bertozzi, and M. A. Lewis, "A nonlocal continuum model for biological aggregation," Bull. Math. Biol. **68**, 1601 (2006).

[8] S. Boi, V. Capasso, and D. Morale, "Modeling the aggregative behavior of ants of the species polyergus rufescens," Nonlinear Anal.: Real World Appl. **1**, 163 (2000).

[9] D. MOrale, V. Capasso, and K. Oelschläger, "An interacting particle system modelling aggregation behavior: from individuals to populations," J. Math. Biol. **50**, 49 (2005).

[10] E. F. Keller and L. A. Segel, "Model for chemotaxis," J. Theor. Biol. **30**, 225 (1971).

[11] M. A. Herrero and J. J. L. Velázquez, "Chemotactic collapse for the Keller-Segel model," J. Math. Biol. **35**, 177 (1996).

[12] F. Filbet, P. Laurencot, and B. Perthame, "Derivation of hyperbolic models for chemosensitive movement," J. Math. Biol. **50**, 189 (2005).

[13] D. D. Holm and V. Putkaradze, "Aggregation of finite-size particles with variable mobility," Phys. Rev. Lett. **95**, 226106 (2005).

[14] D. D. Holm and V. Putkaradze, "Formation of clumps and patches in self-aggregation of finite-size particles," Phys. D **220**, 183 (2006).

[15] D. Benedetto, E. Caglioti, and M. Pulvirenti, "A kinetic equation for granular media," Math. Mod. and Num. An. **31**, 615 (1997).

[16] J. A. Carillo, R. J. McCann, and C. Villani, "Kinetic equilibration rates for granular media and related equations: entropy dissipation and mass transportation estimates," Rev. Mat. Iberoam. **19**, 971 (2003).

[17] J. A. Carillo, R. J. McCann, and C. Villani, "Contractions inthe 2-Wasserstein length space and thermalization of granular media," Arch. Ration. Mech. Anal. **179**, 217 (2006).

[18] H. Li and G. Toscani, "Long-time asymptotics of kinetic models of granular flows," Arch. Ration. Mech. Anal. **172**, 407 (2004).

[19] G. Toscani, "One-dimensional kinetic models of granular flows," Math. Modell. Numer. Anal. **34**, 1277 (2000).

[20] T. Laurent, "Local and global existence for an aggregation equation," Commun. Partial Differ. Equ. **32**, 1941 (2007).

[21] A. L. Bertozzi and T. Laurent, "Finite-time blow-up of solutions of an aggregation equation in $\mathbf{R}^n$," Commun. Math. Phys. **274**, 717 (2007).

[22] A. L. Bertozzi and J. Brandman, "Finite-time blow-up of L^∞-weak solutions of an aggregation equation," Commun. Math. Sci. **8**, 45 (2010).

[23] J. A. Carillo, M. DiFrancesco, A. Figalli, T. Laurent, and D. Slepčev, "Global-in-time weak measure solutions and finite-time aggregation for nonlocal interaction equations," Duke Math. J. **156**, 229 (2011).

[24] J. von Brecht and A. L. Bertozzi, "Well-posedness theory for aggregation sheets," Comm. Math. Phys. (in press).

[25] A. L. Bertozzi, J. A. Carrillo, and T. Laurent, "Blow-up in multidimensional aggregation equations with mildly singular interaction kernels," Nonlinearity **22**, 683 (2009).

[26] A. L. Bertozzi and T. Laurent, "The behavior of solutions of multidimensional aggregation equations with mildly singular interaction kernels," Chin. Ann. Math., Ser. B **30**, 463 (2009).

[27] Y. Huang and A. L. Bertozzi, "Asymptotics of blowup solutions for the aggregation equation," Discrete Contin. Dyn. Syst., Ser. B **17**, 1309 (2012).

[28] F. H. Shu, "Self-similar collapse of isothermal spheres and star formation," in *Bulletin of the American Astronomical Society* **8**, 547 (1976).

[29] J. Silk and Y. Suto, "Stability of collapsing isothermal spheres," Astrophys. J. **335**, 295 (1988).

[30] T. Hanawa and T. Matsumoto, "Stability of dynamically collapsing gas sphere," Publ. Astron. Soc. Jpn. **52**, 241 (2000).

[31] A. J. Bernoff, A. L. Bertozzi, and T. P. Witelski, "Axisymmetric surface diffusion: dynamics and stability of self-similar pinchoff," J. Stat. Phys. **93**, 725 (1998).

[32] M. D. Betterton and M. P. Brenner, "Collapsing bacterial cylinders," Phys. Rev. E **64**, 061904 (2001).

[33] P. M. Lushnikov, "Critical chemotactic collapse," Phys. Lett. A **374**, 1678 (2010).

[34] T. Kolokolnikov, H. Sun, D. Uminsky, J. H. von Brecht, and A. L. Bertozzi, "Ring patterns and their bifurcations in a nonlocal model of biological swarms" (unpublished).

[35] J. H. von Brecht, D. Uminsky, T. Kolokolnikov, and A. L. Bertozzi, "Predicting pattern formation in particle interactions," Math. Mod. Meth. Appl. S. 22 (2012).

[36] J. H. von Brecht and D. Uminsky, "On Soccer Balls and Linearized Inverse Statistical Mechanics," J. Nonlinear Sci. (in press).

[37] H. Cohn and A. Kumar, "Universally optimal distribution of points on spheres," J. Am. Math. Soc. **20**, 99 (2007).

[38] H. Sun, D. Uminsky, and A. L. Bertozzi, "A generalized Birkhoff–Rott equation for two-dimensional active scalar problems," SIAM J. Appl. Math. **72**, 382 (2012).

[39] G. Szego, *Orthogonal polynomials*, 4th edition (American Mathematical Society, Providence, 1939).

[40] T. Kolokolnikov, Y. Huang, and M. Pavlovksy, "Singular patterns for an aggregation model with a confining potential," Physica D (to be published).